PAPER

Highly selective isomerization of cottonseed oil into conjugated linoleic acid catalyzed by multiwalled carbon nanotube supported ruthenium

Shulai Liu, [ID] *[ab] Bokai Yu,[a] Zegao Wang,[de] Jie Hu,[a] Mingwen Fu,[a] Yong Wang,[f] Jianhua Liu, [ID] [a] Zheng Guo,[c] Xuebing Xu[cf] and Yuting Ding*[ab]

Supported ruthenium (Ru) has the capacity to catalyze the conjugation of double bonds in linoleic acid (LA) into conjugated linoleic acids (CLAs). It has been reported that CLAs have shown a lot of benefits to human health. To enhance the selectivity of cottonseed oil (CSO) to CLAs, various Ru catalysts supported by multiwalled carbon nanotubes (Ru/MWCNTs) were prepared using a microwave-heated ethylene glycol method. All catalysts were characterized by transmission electron microscopy (TEM), X-ray diffraction (XRD), X-ray photoelectron spectroscopy (XPS) and inductively coupled plasma optical emission spectrometry (ICP-OES). The catalytic efficiency/selectivity of Ru/MWCNTs and two commercially available Ru catalysts (Ru/C and Ru/Al$_2$O$_3$) were investigated in a solvent-free system by catalyzing the isomerization of CSO. TEM analysis showed that Ru nanoparticles with average sizes of 1.0 nm to 1.8 nm were uniformly dispersed on the surface of the supports. Among the as-synthesized Ru/MWCNTs, catalyst S1 (diameter < 8 nm, length 0.5–2 μm) and catalyst S4 (diameter < 8 nm, length 10–30 μm) exhibit excellent catalytic performance for isomerization of CSO with high yield of total CLA (15.91% and 11.56%, respectively) and high turnover frequency (TOF) of 10.39 and 11.38 h^{-1}, which is much better than two typical commercial Ru catalysts (Ru/Al$_2$O$_3$ and Ru/C). It has been revealed that the average particle size and chemical state of Ru on the surface of MWCNTs have influence on the activity and selectivity of the isomerization reaction.

Introduction

Conjugated linoleic acids (CLAs) are a series of multiple positional (7, 9; 8, 10; 9, 11; 10, 12; 11, 13) and geometrical (*cis* and *trans*) isomers of linoleic acid (LA) containing conjugated double bonds. CLAs are widely found in meat and dairy products of ruminant animals, generated from ruminal biohydrogenation of LA.[1–3] However, only 20 CLAs have been reported in the 54 isomers of CLAs.[4] Among these identified isomers of CLA, it has been proved that the most bioactive forms are *cis*-9, *trans*-11, *trans*-10 and *cis*-12.[5] Recent studies have reported that CLA shows a variety of benefits in improving human health and biological properties, such as anticancer activity,[6] antiobesity effects,[7–9] anti-inflammatory properties,[10] antidiabetic effects,[11] cholesterol lowering[12] and growth promoting.[13]

The main industrial approach to obtaining CLAs is converting LA and their alkyl esters into CLAs by using an alkaline catalyst.[14–16] However, this isomerization process requires a great amount of reagents (alkali bases and solvents (*e.g.* DMSO)), therefore, lacks of ecological efficiency. Moreover, it is impossible to obtain the triglyceride form CLAs directly, and it has been reported that the fatty acids in triglyceride form are easily absorbed in intestine than fatty acid or ethyl ester.[17,18]

It is found that heterogeneous metal catalysts can facilitate the hydrogenation of double bond as well as catalyze the isomerization and double bond conjugation.[15,16,19] Compared with alkaline catalyzed isomerization, heterogeneous metal catalyzed isomerization has a variety of advantages. The process of the heterogeneous metal catalyst based isomerization does not result in a cleavage of ester bond, and the CLA-rich triglycerides can be obtained directly.[20] Besides, the reaction can be carried out under a solvent-free system which can avoid the use of extra reagents.[21] Furthermore, these solid metal-catalysts can be easily separated from the isomerized oil to be reused, and the recycling of the catalysts can thus makes a reduction of cost.

^{a}Department of Food Science, Ocean College, Zhejiang University of Technology, Hangzhou 310014, China. E-mail: slliu@zjut.edu.cn; dingyt@zjut.edu.cn; Fax: +86-571-88320237; Tel: +86-571-88320237

^{b}Institute of Ocean Research, Zhejiang University of Technology, Hangzhou 310032, China

^{c}Department of Engineering, Faculty of Science and Technology, Aarhus University, 8000 Aarhus C, Denmark

^{d}College of Materials Science and Engineering, Sichuan University, Chengdu 610065, China

^{e}Interdisciplinary Nanoscience Center, Aarhus University, 8000 Aarhus C, Denmark

^{f}Wilmar (Shanghai) Biotechnology Research & Development Center Co. Ltd, Area A, Shanghai 200137, China

So far a lot of metal catalysts have shown the potential to conjugate the unsaturated fatty acid. Among these catalysts, ruthenium based catalysts display a remarkable performance in the conjugation of LA.[21–24] Besides, the nature of the supports is another important factor which affects the catalytic performance of metal catalysts. As reported in the literatures, a variety of materials (such as activated carbon, alumina and zeolite) have been used as supports for loading metals for LA isomerization to synthesize CLA.[22,25–27] Most of the works in the literatures use LA and its esters as substrates, which can not obtain CLA-rich triglycerides by one step. Moreover, low selectivity of CLA is another drawback.

Above all, it's meaningful for industrial production of CLA to synthesize a better catalyst with high catalytic activity and high selectivity of bioactive CLA forms. Since the tubular carbon structures was first time observed by Iijima in 1991,[28] carbon nanotubes (CNTs) have been extensively studied. CNTs exhibited many excellent properties as a support in catalysis in many literatures, such as low corrosion, resistance to acid or alkali, high thermal (under inert atmospheres) and mechanical stability, possibility of affecting the activity and selectivity by tuning the specific metal-support interactions and lower cost compared with conventional supports like alumina or silica.[29–32] Due to the excellent catalytic performance of CNTs, metal supported on catalysts were widely studied in many literatures.[33,34]

However, there is few literatures about carbon nanotubes catalysts used for LA isomerization into CLA. In this view, this work investigated the LA isomerization into CLA over ruthenium supported on multi-walled carbon nanotubes (MWCNTs) catalysts (Ru/MWCNTs). The ruthenium chloride hydrate and six MWCNTs with different length and diameter were used as catalyst precursors and supports to synthesize Ru/MWCNTs catalysts respectively. The synthesis of Ru/MWCNTs catalysts was carried out in ethylene glycol (EG) with the assistance of microwave heating. Besides, to better guide the industrial production of CLA, the refined cottonseed oil (CSO which contains about 55% of LA) was selected as the reaction substrate in this work, so that CLA-rich triglycerides can be obtained directly. To compare the catalytic performance with existing commercial catalysts, the synthesized Ru/MWCNTs catalysts were compared with two typically commercial catalysts, which are reported mostly in the literatures, and the results showed that excellent catalytic activity and selectivity in LA conjugation of CSO.

Materials and methods

Materials

Carboxylic MWCNTs was obtained from Dekedaojing Corporation (Beijing, China). Ruthenium chloride hydrate (35.0–42.0% Ru basis) was purchased from Aladdin industrial Corporation (Shanghai, China). Ruthenium 5% on alumina (Ru/Al₂O₃) and ruthenium 5% on activated charcoal (Ru/C) were supplied by Sigma-Aldrich Co. (St. Louis, MO, USA). LA (≥99.0% purity based on GC analysis) was purchased from Aladdin industrial Corporation (Shanghai, China). Refined CSO was donated by Wilmar Biotechnology Research & Development Center

(Shanghai) Co., Ltd (Shanghai, China). Boron trifluoride-methanol solution (15% BF_3 in methanol) and *n*-decane were purchased from Sigma-Aldrich Co. (St. Louis, MO, USA). All chemicals and solvents were of analytical grade.

Synthesis of Ru/MWCNTs catalysts

Ruthenium loading on all Ru/MWCNTs catalysts are theoretically 5%. Typically, 0.2 g MWCNTs was added in 120 mL ethylene glycol. And the mixture was under sonication for 30 min to make sure MWCNTs are uniformly dispersed. After sonication, 3.0 mL of aqueous $RuCl_3 \cdot xH_2O$ solution was added dropwise with continuous stirring for 30 min. And then the 1 mol L^{-1} NaOH ethylene glycol solution was used to adjust the pH of the mixture to 4.0. Then, the solution was put in a microwave synthesis reactor to heated for 100 s (800 W) after continuous stirring for 24 h. The mixture solution was filtered, washed with deionized water until the pH of the filtrate reached the value 7.0, and dried at 80 °C under vacuum overnight. The sample was ground to powder to use.

Characterization

Transmission electron microscope (TEM) images of samples were obtained by using a FEI Tecnai G2 F20. X-ray diffraction (XRD) of samples was obtained on a PNAlytical X' Pert PRO X-ray powder diffractometer, Cu Kα radiation was employed and the working voltage and current were 60 kV and 55 mA, respectively. X-ray photoelectron spectroscopy (XPS) was performing using Kratos AXIS Ultra DLD with Al Kα radiation. Inductively coupled plasma optical emission spectrometry (ICP-OES) was carried out on a SPECTRO ARCOS MV to obtain the content of ruthenium in catalysts.

Isomerization reaction

The reaction method was modified from the procedure of Liu *et al.*[21] Isomerization of LA and CSO was carried out in a 10 mL pressure-resistant tube reactor (supplied by Sytracks Aps C/o, Interdisciplinary Nanoscience Center, Aarhus, Denmark) at 165 °C (thermo-controlled by an oil-bath) with constant stirring (800 rpm). In a typical experiment, 0.025 g catalyst and 1.0 g CSO were used. The reactor was loaded with the catalyst and the substrate followed by purging with nitrogen for 2 min. The reaction reactor containing substrate and catalyst was then heated to the designated temperature with continuous magnetic stirring.

GC-MS analysis of fatty acid composition

The isomerized LA and CSO were methylated *via* alcoholysis in the presence of 0.5 mol L^{-1} methanolic NaOH solution for 5 min and 15% BF_3 in methanol for 2 min at 80 °C. The resulting fatty acid methyl esters (FAME) were rinsed by saturated NaCl–K_2CO_3 aqueous solution. The solution was then extracted with *n*-hexane, and the organic layer was dried over anhydrous Na_2SO_4. FAME compositions were analyzed by gas chromatography-mass spectrometer (GC-MS, Thermo Scientific, Shanghai, China) equipped with a fused silica capillary

column (0.25 mm, 0.2 μm, 100 m, Supelco), using helium gas as the carrier at flow rate of 1.0 mL min^{-1}. The temperature of the column was held at 170 °C for 1.0 min; then increased to 195 °C at the rate of 0.8 °C min^{-1} and kept for 12 min; followed by increasing at the rate of 5 °C min^{-1} to 220 °C and kept for 1 min. The temperatures of the injector and the FID detector were set at 250 °C. Area% was converted to wt% using FID response factors described in AOCS Ce 1f-96, and then to mol% calculated by being divided their corresponding molecular weights. In order to quantify the catalytic efficiency of the catalysts, the conversion of LA (X_{LA}) is used to denote the catalytic activity. To characterize the catalytic specificity towards different products, S_{CLA}, S_{ct}, S_{tt}, were used to represent reaction selectivity towards the formation of total CLA, *cis*-9, *trans*-11- + *trans*-10, *cis*-12-CLA and *trans*-9, *trans*-11 + *trans*-10, *trans*-12-CLA. Y_{CLA} stands for the yield (content in product mixture) of total CLA.[16]

$$X_{LA} = \frac{LA_0 - LA_1}{LA_0} \quad (1)$$

$$Y_{CLA} = CLA_1 - CLA_0 \quad (2)$$

$$S_{CLA} = \frac{CLA_1 - CLA_0}{LA_0 - LA_1} \quad (3)$$

$$S_{ct} = \frac{(c,t\text{-}CLA)_1 - (c,t\text{-}CLA)_0}{LA_0 - LA_1} \quad (4)$$

$$S_{tt} = \frac{(t,t\text{-}CLA)_1 - (t,t\text{-}CLA)_0}{LA_0 - LA_1} \quad (5)$$

where LA_0; CLA_0; $(c,t\text{-}CLA)_0$; $(t,t\text{-}CLA)_0$ represent the content (%) of LA; total CLA; c,t-CLA (*cis*-9, *trans*-11- + *trans*-10, *cis*-12-CLA); t,t-CLA (*trans*-9, *trans*-11- + *trans*-10, *trans*-12-CLA) in CSO. LA_1; CLA_1; $(c,t\text{-}CLA)_1$; $(t,t\text{-}LA)_1$ represent the content (%) of LA; total CLA; c,t-CLA (*cis*-9, *trans*-11- + *trans*-10, *cis*-12-CLA); t,t-CLA (*trans*-9, *trans*-11- + *trans*-10, *trans*-12-CLA) in conjugated products of CSO.

Results and discussion

Characterization of Ru/MWCNTs catalysts

Since the surface of MWCNTs is hydrophobic, they tend to aggregate in polar solvent. And the MWCNTs modified by functional groups can provide enough defects to make ruthenium nanoparticles uniformly distribute on its surface of MWCNTs. In this work, MWCNTs modified with carboxyl (shown in Table 1) with different length and diameter were

chosen as the supports. The corresponding catalysts are represented as S1, S2, S3, S4, S5 and S6. The MWCNTs supported Ru nanoparticles (NPs) were prepared by a microwave-heated polyol process. It has been agreed by a large number of studies that the microwave-heated polyol process is an efficient way to prepare polymer stabilized metal nanoparticles.[35–38] The synthesis process is shown in Fig. 1.

Transmission electron microscopy (TEM) analysis reveals that the Ru NPs in the Ru/MWCNTs catalysts (Fig. 2) uniformly dispersed on the surface of the supports and have a narrow distribution in average size of 1.0 to 1.8 nm. The particle size distribution are estimated based on 200 particles selected randomly for each catalyst. It is generally agreed that the rate of reduction of the metal precursor determines the size of metal NPs. Due to the high dielectric constant (41.4 at 298 K) and the dielectric loss of ethylene glycol, the rapid heating can occur easily under microwave irradiation. Fast heating rates can accelerate the formation of the metal NPs, and the uniform microwave irradiation provides more homogeneous circumstances for their nucleation growth. Fig. 2 also shows that the average Ru particle sizes of Ru/Al$_2$O$_3$ and Ru/C are 1.4 nm and 1.2 nm, respectively.

Fig. 3 shows XRD patterns of raw materials of MWCNTs (a) and Ru/MWCNTs catalysts (b). The raw materials of MWCNTs exhibits 3 peaks at 26.0°, 43.0° and 44.5°, corresponding to the (002), (100), and (101) planes of graphite,[39] respectively. Intriguingly, there is no obvious difference between the Fig. 3(a) and (b), which means that the diffraction signals related to the Ru species can not be observed from XRD. This phenomenon confirms that ruthenium has a good deposition on the surface of MWCNTs. Besides, the TEM results show that the average size of Ru NPs is less than 1.8 nm (1.0–1.8 nm). It is generally believed that the XRD diffraction peak broadens with the decrease of the nanoparticle size. Moreover, when the size of Ru crystallites is lower than the limitation of XRD detection, the diffraction peak cannot be observed. The result of XRD is consistent with the TEM results.

X-ray photoelectron spectroscopy (XPS) is generally used to identify the composition and chemical states of the components on the surface of materials.[40] In order to observe and analyze the oxidation states and content of ruthenium in the catalysts, the XPS analysis is performed for different Ru/MWCNTs catalysts. It can be obviously seen from Fig. 4 that the dominant composing elements are C, O and Ru for six Ru/MWCNTs catalysts. The two characteristic B.E. peaks at around 483–487 eV and 461–467 eV are contributed to 3p$_{1/2}$ and 3p$_{3/2}$,

Table 1 The properties of six types of MWCNTs supports

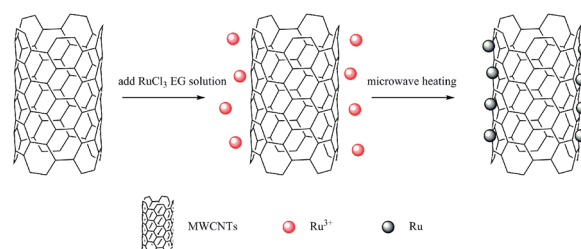| MWCNTs	Diameter (nm)	Length (μm)	Specific surface area (m^2 g^{-1})	–COOH (wt%)
1	<8	0.5–2	>500	3.86
2	10–20	0.5–2	>200	3.86
3	>50	0.5–2	>40	3.86
4	<8	10–30	>500	3.86
5	10–20	10–30	>200	3.86
6	>50	10–30	>40	3.86

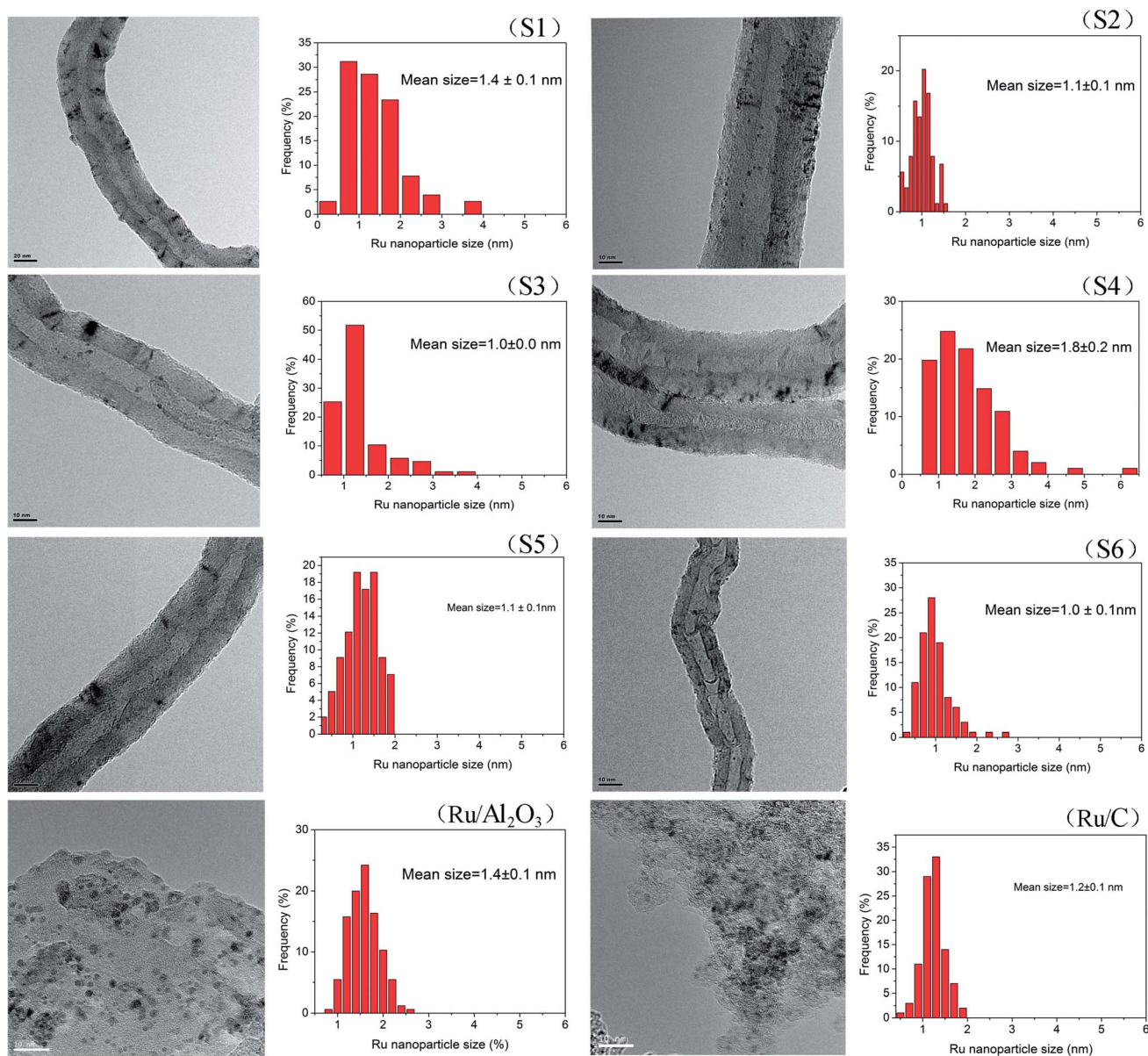**Fig. 1** Synthesis process of Ru/MWCNTs catalysts.

Fig. 2   TEM images and crystal size distribution of different Ru/MWCNTs catalysts and two commercial Ru catalysts.

respectively. The C 1s peak is overlapped with Ru 3d peak at around 284 eV. To obtain the information of Ru oxidation states, we have performed the deconvolution of 3p peaks (Fig. 5, calibrated by C 1s) by with 80% Gaussian and 20% Lorentzian fitting. To avoid the interference from carbon substrate the
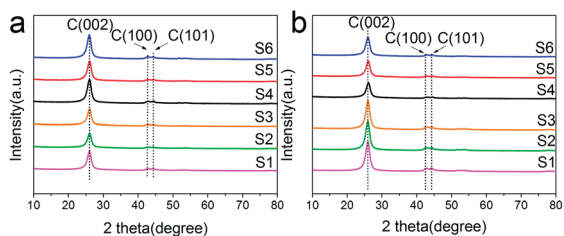

Fig. 3   XRD patterns of MWCNTs supports (a) and Ru/MWCNTs catalysts (b).

deconvolution of 3d spectra is not performed (Fig. 6).[41] For comparison purpose, all peaks are deconvoluted into two components: $RuO_2(IV)$ and $Ru(0)$. The detailed analysis results of atomic composition and Ru oxidation state are shown in Table 2. Besides, the signal of Ru 3p of S2 catalyst from Fig. 5(b) is not observed, which might be due to the content of Ru is lower than the limitation of XPS. As shown from Table 2, the atomic ratio of Ru ranges from 0.18% to 0.58%; and the different ruthenium loading of six Ru/MWCNTs catalysts may contribute to the physical properties (diameter and length) of the support are different, which may influence the reduction of ruthenium nanoparticles. Moreover, it can be found that the atomic ratio of ruthenium of S1 catalysts is higher than S2 and S3 catalysts which has the same length (0.5–2μm) but different diameter (S1 < 8 nm, S2 10–20 nm, S3 > 50 nm); and this phenomenon also can be seen in S4, S5, S6 catalysts whose
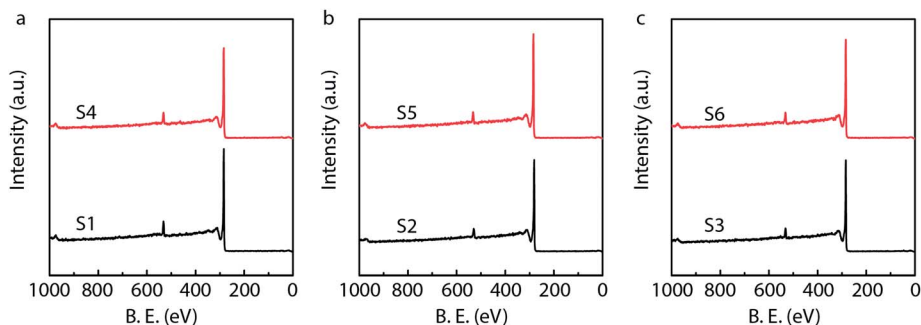
Fig. 4 XPS spectra of different Ru/MWCNTs catalysts.

length is 10–30 μm. To obtain the Ru content of different catalysts, the ICP-OES was performed (shown in Table 2). The ICP-OES results show that the ruthenium contents for S1 to S6 catalyst are 2.8%, 1.1%, 2.0%, 1.9%, 1.5%, 1.6% respectively, and Ru/Al$_2$O$_3$ and Ru/C are 4.9% and 4.9% respectively.

Isomerization reaction results of cottonseed oil with Ru/MWCNTs catalysts

In current work we choose two typical commercial catalysts (Ru/Al$_2$O$_3$ and Ru/C) to isomerize CSO for comparison. The isomerization reaction results are shown in Table 3. According to previous work, 165 °C was chosen as the reaction temperature and 800 rpm stirring rate is used to assure the catalysts disperse uniformly in the substrate.[21]

As seen from Table 3, the conversion of LA in CSO (X_{LA}) of six Ru/MWCNTs catalysts (S1 to S6) ranges from 7.93% to 37.66%; the yield of total CLA (Y_{CLA}) of six Ru/MWCNTs ranges from 2.25% to 15.91%. Especially, sample 1 (S1) shows the best catalytic activity both in X_{LA} (37.66%) and Y_{CLA} (15.91%); which is much higher than Ru/Al$_2$O$_3$ (X_{LA} 5.57% and Y_{CLA} 1.95%) and Ru/C (X_{LA} 14.21% and Y_{CLA} 5.82%). The selectivity towards CLA (S_{CLA}) and selectivity towards cis-9, trans-11- and 10-trans, cis-12-CLAs (S_{ct}) of six Ru/MWCNTs are 49.56–74.34% and 44.05–65.63%, respectively. Except S5 (S_{CLA} 49.56% and S_{ct} 44.05%), the selectivity towards CLA and the selectivity towards cis-9, trans-11- and 10-trans, cis-12-CLA of Ru/MWCNTs catalysts are higher than Ru/Al$_2$O$_3$ (S_{CLA} 61.13% and S_{ct} 52.98%). Compared with Ru/C (S_{CLA} 71.50% and S_{ct} 62.65%), there is no significant difference in S_{CLA} and S_{ct} of Ru/MWCNTs (except S5).

The nature of the support materials and the redox states of the metal are known to influence the chemisorptive and affect

the catalytic properties of metal catalyst.[42] Combine the XPS and the isomerization reaction result, it can be found that the ratio of Ru(0) and Ru(IV) of S1 (Ru(0) 49% and Ru(IV) 51%) and S4 (Ru(0) 51% and Ru(IV) 49%), which have higher Y_{CLA}, is more closer to 1 : 1. It also can be seen from other catalysts including S3 (Ru(0) 53% and Ru(IV) 47%), S5 (Ru(0) 47% and Ru(IV) 53%), S6 (Ru(0) 48% and Ru(IV) 52%), Ru/Al$_2$O$_3$ (Ru(0) 44% and Ru(IV) 56%) and Ru/C (Ru(0) 53% and Ru(IV) 47%) when the ratio of Ru(0) and Ru(IV) is far away from 1 : 1, the Y_{CLA} decreases. And the S3 and Ru/C with same ratio of Ru(0) and Ru(IV) show the similar isomerization result. All the Ru/MWCNTs exhibited better catalytic performance than Ru/C and Ru/Al$_2$O$_3$, this can be contributed to metal-support interaction. As literatures reported,[43] the MWCNTs can transfer electron to Ru which can increase the chance of substrate and metal contact to obtain better catalytic activity.

The isomerization process of LA into CLA can be explained by the Horiuti–Polanyi mechanism, which describes hydrogenation and isomerization of olefins. As shown in Fig. 7, there are several steps: (a) linoleic acid is chemisorbed on the Ru surface. (b) A hydrogen atom desorbs from Ru surface formatting a half-hydrogenated intermediate. (c) The formation of a saturated bond or (d) Abstraction of a neighbouring hydrogen leading to the formation of a di-adsorbed complex. (e) The desorption of the geometrical and/or positional isomer. When the adsorbed hydrogen on the Ru surface is high, the hydrogenation of half-hydrogenated intermediate will happen (step (c)). In this work, the catalysts were not preactivated by H$_2$ making the adsorbed hydrogen on the Ru surface is low, making reaction trend to isomerization not hydrogenation. Furthermore, due to the electron-donor property of MWCNTs,
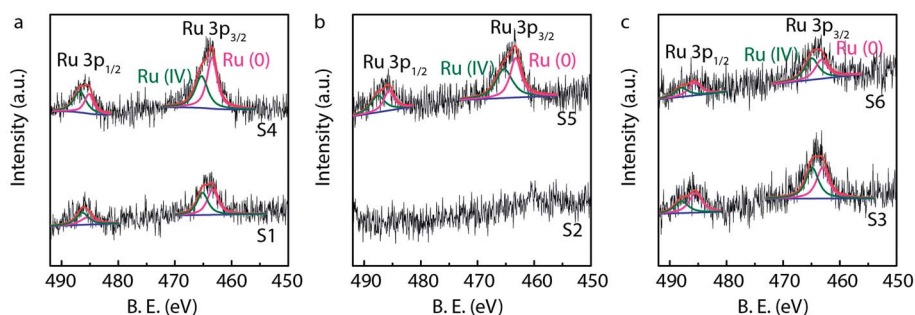

Fig. 5 High resolution Ru 3p XPS spectra of Ru/MWCNTs catalysts with analysis of oxidation states and atomic ratio of Ru.
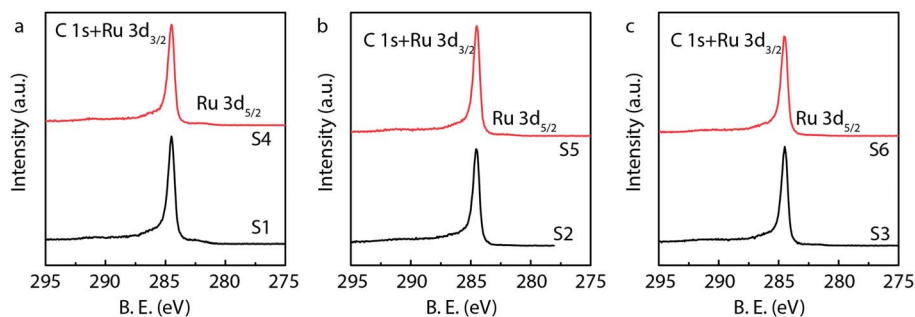
Fig. 6 High resolution C 1s and Ru 3d XPS spectra of Ru/MWCNTs catalysts.

Table 2 Spectral parameters for XPS of different supported Ru catalysts

| Catalyst | State | Ru 3p B.E. | | | Atomic ratio (%) | | | | Ru (wt%) |
		3/2	1/2	%	C	O	Na	Ru	
S1	0	463.36	485.39	49	94.56	4.89	0.19	0.35	2.8
	IV	465.13	486.34	51					
S2	0	—	—	—	95.32	4.53	0.15	—	1.1
	IV	—	—	—					
S3	0	463.05	485.46	53	95.45	4.16	0.14	0.25	2.0
	IV	464.89	487.96	47					
S4	0	463.44	485.15	51	94.96	4.69	0.12	0.23	1.9
	IV	465.31	486.76	49					
S5	0	463.26	485.63	47	95.44	4.27	0.11	0.18	1.5
	IV	465.30	487.62	53					
S6	0	463.26	485.60	48	95.54	4.14	0.12	0.20	1.6
	IV	464.97	488.00	52					
Ru/Al$_2$O$_3$ (ref. 21)	0	462.88	485.63	44	—	67.2	—	2.2	4.9
	IV	464.96	489.15	56					
Ru/C[21]	0	462.61	483.41	53	96.3	8.1	—	5.6	4.9
	IV	464.79	485.85	47					

there is a metal-support interaction between Ru nanoparticles and MWCNTs, which prevents the re-oxidation of Ru and increases the chance of linoleic acid and Ru contact to obtain better conjugation results.[43] This can be used for the explanation of why all the Ru/WMCNTs exhibited better catalytic performance than Ru/C and Ru/Al$_2$O$_3$.

To compare the catalytic properties over different catalysts, the calculation results of the number of moles of ruthenium in catalysts (in 25 mg catalyst), conversion of LA (X_{LA}) and turnover

Table 3 Selectivity in linoleic acid of cottonseed oil isomerization over different catalysts[a]

Catalyst	T (°C)	Y_{CLA} (%)	X_{LA} (%)	S_{CLA} (%)	S_{ct} (%)	S_{tt} (%)
S1	165	15.91	37.66	73.76	59.02	14.74
S2	165	5.23	12.80	71.35	63.17	8.19
S3	165	6.23	14.63	74.34	65.63	8.71
S4	165	11.56	28.53	70.75	58.75	12.00
S5	165	2.25	7.93	49.56	44.05	5.51
S6	165	6.99	17.84	68.40	59.20	9.20
Ru/Al$_2$O$_3$	165	1.95	5.57	61.13	52.98	8.15
Ru/C	165	5.82	14.21	71.50	62.65	8.85

[a] Reaction conditions: substrate load, 1 g of cottonseed oil; reaction time: 8 h; catalyst load, 0.025 g.

frequency of CLA (TOF$_{CLA}$) were shown in Table 4. Among the remaining seven catalysts, sorting results by TOF$_{CLA}$ is S4 > S1 > S3 > S5 > S6 > Ru/C > Ru/Al$_2$O$_3$. Besides, the TOF$_{CLA}$ of sample 4 (11.38 h^{-1}) and sample 1 (10.39 h^{-1}) are much higher than two commercial catalysts (Ru/Al$_2$O$_3$ 0.72 h^{-1} and Ru/C 2.14 h^{-1}). In addition to high TOF of S1 and S4 catalysts, X_{LA} of S1 (21.57%) and S4 (16.34%) is also much higher than other catalysts. Compared with other catalysts, the supports of S1 catalyst and S4 catalyst have bigger specific surface area (shown in Table 1). As literatures said, higher specific surface area may supports more active sites which can increase catalytic activity.[44–46] Although the TOF$_{CLA}$ of S2 with low ruthenium loading is up to 8.76 h^{-1}, the Y_{CLA} and X_{LA} are just 5.23% and 7.33% respectively. Furthermore, if the left several samples were sorting by average size, the order is S4 (1.8 nm) > S1 (1.4 nm) > S3 (1.3 nm) > S5 (1.1 nm) > S6 (1.0 nm), which is well consistent with TOF sort result; and from this result, the size of Ru nanoparticles may influence the TOF of the reaction.

In selectivity aspect (data was shown in Table 3), it is found that high X_{LA} is always with high yield of CLA (Y_{CLA}) and high selectivity of *trans*, *trans*-CLA (S_{tt}). This is due to the consumption of LA is a second-order reaction and that the rate of consumption of LA depends on the concentration of LA present in the reaction system, and the formation of *trans*, *trans*-CLA is
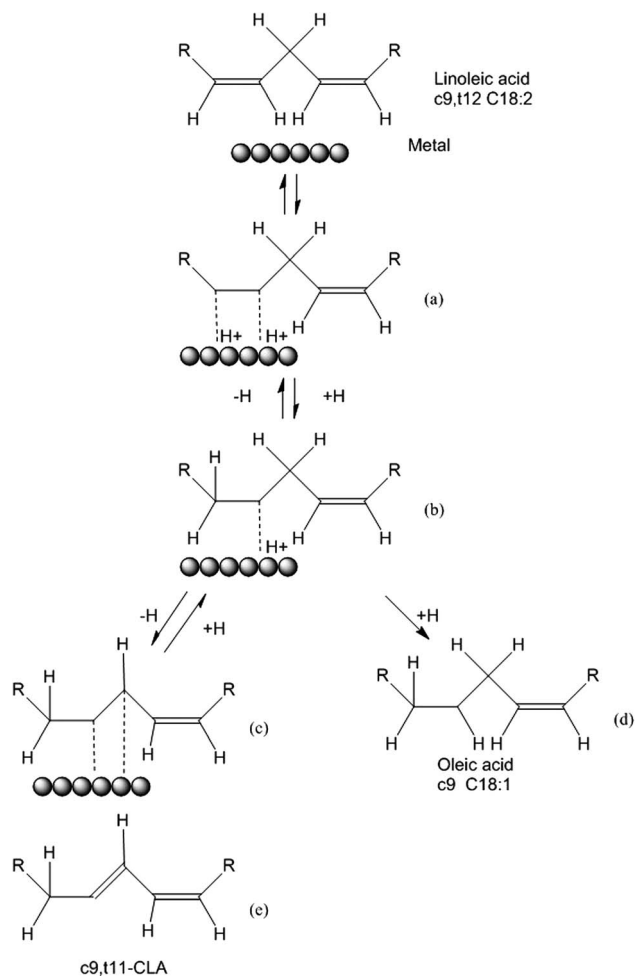
Fig. 7 Horiuti–Polanyi mechanism of the isomerization and hydrogenation of linoleic acid.

Table 4 Comparison of different catalysts for linoleic acid conjugation

Catalyst	Y_{CLA} (%)	n_{Ru} (mol)	X_{LA} (%)	$TOF_{CLA}{}^{a}$ (h^{-1})
S1	15.91	6.98×10^{-6}	21.57	10.39
S2	5.23	2.72×10^{-6}	7.33	8.76
S3	6.23	5.05×10^{-6}	8.28	5.62
S4	11.56	4.63×10^{-6}	16.34	11.38
S5	2.25	3.64×10^{-6}	4.54	2.81
S6	6.99	1.14×10^{-6}	10.22	2.79
Ru/Al$_2$O$_3$	1.95	1.24×10^{-5}	3.19	0.72
Ru/C	5.82	1.24×10^{-5}	8.14	2.14

^{a} TOF_{CLA} = mole of total CLA/(moles of surface Ru × reaction times). Moles of surface Ru was calculated.

governed by thermodynamics.[47,48] Though there is no obvious advantage in selectivity of total CLA and *cis*, *trans*-CLA compared with two commercial catalysts, what should be noticed is that the two commercial catalysts stay in low X_{LA} while the X_{LA} of S1 and S4 is up to 37.66% and 28.53% respectively. In this work, the oxidation state of Ru (shown in Table 2) doesn't display a significant influence on selectivity of products over isomerization of CSO.

Conclusions

In summary, a series of novel Ru/MWCNTs catalysts have been successfully prepared with the assistance of microwave heating in ethylene glycol. It has been determined that the small size of Ru nanoparticles are highly dispersed on the surface of mutiwalled carbon nanotubes. The TEM and TOF results revealed that higher TOF is always with higher average size of Ru NPs. The analysis of isomerization and XPS shows the redox state of Ru can affect isomerization reaction. Among the as-synthesized Ru/MWCNTs, S1 catalyst (diameter < 8 nm, length 0.5–2 μm) and S4 catalyst (diameter < 8 nm, length 10–30 μm) exhibit excellent catalytic performance for isomerization of cottonseed oil with high yield of total CLA (15.91% and 11.56%, respectively) and high TOF values of 10.39 and 11.38 h^{-1}, which is far better than two typically commercial Ru catalysts (Ru/Al$_2$O$_3$ and Ru/C). In addition, the isomerization catalyzed by Ru/MWCNTs keeps high selectivity of *cis*, *trans*-CLA (around 70%) with high yield of total CLA.

Conflicts of interest

There are no conflicts to declare.

Acknowledgements

Notes and references

1 C. M. Alfaia, S. P. Alves, J. M. Pestana, M. S. Madeira, O. Moreira, J. Santos-Silva, R. J. B. Bessa, F. Toldra and J. A. M. Prates, *Food Sci. Technol. Int.*, 2017, **23**, 209–221.
2 S. Banni, *Curr. Opin. Lipidol.*, 2002, **13**, 261–266.
3 R. J. B. Bessa, S. P. Alves, E. Jeronimo, C. M. Alfaia, J. A. M. Prates and J. Santos-Silva, *Eur. J. Lipid Sci. Technol.*, 2007, **109**, 868–878.
4 P. Delmonte, J. A. G. Roach, M. M. Mossoba, G. Losi and M. P. Yurawecz, *Lipids*, 2004, **39**, 185–191.
5 M. W. Pariza, Y. Park and M. E. Cook, *Prog. Lipid Res.*, 2001, **40**, 283–298.
6 N. S. Kelley, N. E. Hubbard and K. L. Erickson, *J. Nutr.*, 2007, **137**, 2599–2607.
7 C. Druart, E. M. Dewulf, P. D. Cani, A. M. Neyrinck, J. P. Thissen and N. M. Delzenne, *Lipids*, 2014, **49**, 397–402.
8 A. Kennedy, K. Martinez, S. Chung, K. LaPoint, R. Hopkins, S. F. Schmidt, K. Andersen, S. Mandrup and M. McIntosh, *J. Lipid Res.*, 2010, **51**, 1906–1917.
9 N. M. Racine, A. C. Watras, A. L. Carrel, D. B. Allen, J. J. McVean, R. R. Clark, A. R. O'Brien, M. O'Shea, C. E. Scott and D. A. Schoeller, *Am. J. Clin. Nutr.*, 2010, **91**, 1157–1164.
10 M. Flowers and P. A. Thompson, *PLoS One*, 2009, **4**, 9.
11 N. Castro-Webb, E. A. Ruiz-Narvaez and H. Campos, *Am. J. Clin. Nutr.*, 2012, **96**, 175–181.

12 I. J. Onakpoya, P. P. Posadzki, L. K. Watson, L. A. Davies and E. Ernst, *Eur. J. Nutr.*, 2012, **51**, 127–134.

13 L. Rainer and C. J. Heiss, *J. Am. Diet. Assoc.*, 2004, **104**, 963–968.

14 Z. Guo, G. W. Zhang and Y. Sun, *Chin. J. Chem. Eng.*, 2003, **11**, 130–135.

15 A. Philippaerts, S. Goossens, P. A. Jacobs and B. F. Sels, *ChemSusChem*, 2011, **4**, 684–702.

16 A. Philippaerts, S. Goossens, W. Vermandel, M. Tromp, S. Turner, J. Geboers, G. Van Tendeloo, P. A. Jacobs and B. F. Sels, *ChemSusChem*, 2011, **4**, 757–767.

17 Z. Guo and Y. Sun, *Food Chem.*, 2007, **100**, 1076–1084.

18 J. Neubronner, J. P. Schuchardt, G. Kressel, M. Merkel, C. von Schacky and A. Hahn, *Eur. J. Clin. Nutr.*, 2011, **65**, 247–254.

19 M. Kreich and P. Claus, *Angew. Chem., Int. Ed.*, 2005, **44**, 7800–7804.

20 P. Pakdeechanuan, K. O. Intarapichet, L. N. Fernando and I. U. Grun, *J. Agric. Food Chem.*, 2005, **53**, 923–927.

21 S. Liu, Z. Wang, X. Xu, Y. Ding and Z. Guo, *Ind. Crops Prod.*, 2017, **97**, 10–20.

22 A. Bernas, N. Kumar, P. Maki-Arvela, N. V. Kul'kova, B. Holmbom, T. Salmi and D. Y. Murzin, *Appl. Catal., A*, 2003, **245**, 257–275.

23 A. Bernas, P. Maki-Arvela, N. Kumar, B. Holmbom, T. Salmi and D. Y. Murzin, *Ind. Eng. Chem. Res.*, 2003, **42**, 718–727.

24 N. Chorfa, S. Hamoudi and K. Belkacemi, *Appl. Catal., A*, 2010, **387**, 75–86.

25 A. Bernas, P. Laukkanen, N. Kumar, P. Maki-Arvela, J. Vayrynen, E. Laine, B. Holmbom, T. Salmi and D. Y. Murzin, *J. Catal.*, 2002, **210**, 354–366.

26 O. A. Simakova, A.-R. Leino, B. Campo, P. Maki-Arvela, K. Kordas, J.-P. Mikkola and D. Y. Murzin, *Catal. Today*, 2010, **150**, 32–36.

27 V. M. Deshpande, R. G. Gadkari, D. Mukesh and C. S. Narasimhan, *J. Am. Oil Chem. Soc.*, 1985, **62**, 734–738.

28 S. Iijima, *Nature*, 1991, **354**, 56–58.

29 S. A. Chernyak, E. V. Suslova, A. V. Egorov, L. Lu, S. V. Savilov and V. V. Lunin, *Fuel Process. Technol.*, 2015, **140**, 267–275.

30 E. Perez-Mayoral, V. Calvino-Casilda and E. Soriano, *Catal. Sci. Technol.*, 2016, **6**, 1265–1291.

31 C. Pham-Huu, N. Keller, V. V. Roddatis, G. Mestl, R. Schlogl and M. J. Ledoux, *Phys. Chem. Chem. Phys.*, 2002, **4**, 514–521.

32 P. Serp and E. Castillejos, *ChemCatChem*, 2010, **2**, 41–47.

33 R. M. M. Abbaslou, A. Tavassoli, J. Soltan and A. K. Dalai, *Appl. Catal., A*, 2009, **367**, 47–52.

34 P. Serp, M. Corrias and P. Kalck, *Appl. Catal., A*, 2003, **253**, 337–358.

35 W. X. Chen, J. Zhao, J. Y. Lee and Z. L. Liu, *Mater. Chem. Phys.*, 2005, **91**, 124–129.

36 S. Komarneni, D. S. Li, B. Newalkar, H. Katsuki and A. S. Bhalla, *Langmuir*, 2002, **18**, 5959–5962.

37 Z. L. Liu, J. Y. Lee, W. X. Chen, M. Han and L. M. Gan, *Langmuir*, 2004, **20**, 181–187.

38 W. Y. Yu, W. X. Tu and H. F. Liu, *Langmuir*, 1999, **15**, 6–9.

39 B. D. Li, C. Wang, G. Q. Yi, H. Q. Lin and Y. Z. Yuan, *Catal. Today*, 2011, **164**, 74–79.

40 E. A. Paoli, F. Masini, R. Frydendal, D. Deiana, C. Schlaup, M. Malizia, T. W. Hansen, S. Horch, I. E. L. Stephens and I. Chorkendorff, *Chem. Sci.*, 2015, **6**, 190–196.

41 B. Şen, B. Demirkan, A. Savk, R. Kartop, M. S. Nas, M. H. Alma, S. Sürdem and F. Şen, *J. Mol. Liq.*, 2018, **268**, 807–812.

42 C. Elmasides, D. I. Kondarides, W. Grunert and X. E. Verykios, *J. Phys. Chem. B*, 1999, **103**, 5227–5239.

43 F. Salman, C. Park and R. T. K. Baker, *Catal. Today*, 1999, **53**, 385–394.

44 F. L. Yang, J. Ren, Q. Q. Liu, L. Zhang, Y. Y. Chai and W. L. Dai, *J. Energy Chem.*, 2019, **33**, 1–8.

45 Y. X. Wang, S. Aghamohammadi, D. Y. Li, K. Z. Li and R. Farrauto, *Appl. Catal., B*, 2019, **244**, 438–447.

46 L. M. Zhu, Z. H. Wang, L. Wang, L. L. Xie, J. J. Li and X. Y. Cao, *Chem. Eng. J.*, 2019, **364**, 503–513.

47 Q. Guo, F. He, Q. Li, Z. Deng, J. Jin and Y. Ha, *Food Control*, 2016, **67**, 255–264.

48 M. Q. Xu, S. S. Wang, L. N. Li, J. Gao and Y. W. Zhang, *Catalysts*, 2018, **8**, 460–479.